Photodissociation Spectroscopy of Zn^+−Methanol

W.-Y. Lu, T.-H. Wong, Y. Sheng, A. T. Lytle, and P. D. Kleiber*

Department of Physics and Astronomy, University of Iowa, Iowa City, Iowa 52242

Received: September 9, 2002; In Final Form: November 25, 2002

We report on studies of the photodissociation spectroscopy of Zn^+−methanol complexes in the near-UV region. We observe two absorption bands assigned to Zn^+-based 4p ← 4s transitions in a C_s Zn^+−$OHCH_3$ association complex. The $2^2A'(4p\pi) \leftarrow 1^2A'(4s\sigma)$ band shows a significant vibronic resonance structure that can be assigned to a combination of both inter- and intramolecular vibrational modes of the complex. The experimental vibrational frequencies are in excellent agreement with the theoretical model predictions. The higher-energy $2^2A''(4p\pi) \leftarrow 1^2A'(4s\sigma)$ band is strongly coupled to a lower lying charge-transfer state and appears as a structureless continuum. We observe very little reactive branching; rather, charge transfer to $CH_3OH^+ + Zn$ products dominates the dissociation. These results are compared with previous studies of other main-group- and transition-metal-ion−methanol complexes.

I. Introduction

Metal-ion−methanol complexes have been the subject of several recent spectroscopic studies.[1−7] Methanol is a polar solvent, and the photodissociation spectroscopy of mass-selected metal-ion−methanol clusters allows a study of the stepwise effects of increasing the solvation on the electronic structure of the chromophore and intracluster reactivity, giving information about the transition from the gas-phase to the solution-phase limit.[1−4] More recently, transition-metal-ion−methanol complexes have been used as precursors for the study of reactive intermediates in the conversion of methane to methanol by metal oxide cation molecules or on bulk metal oxide surfaces.[5]

Farrar and co-workers have studied the photodissociation of $Sr^+(CH_3OH)$ and $Sr^+(CH_3OD)$ in the visible region, observing both the evaporation product Sr^+ and reaction products $SrOH^+$ and $SrOD^+$.[1] In the highest-energy Sr^+-based $5p\pi-5s\sigma$ transition, the reaction yield was very high, ∼90%. The lower-energy bands, assigned to Sr^+-based 4d−5s transitions, show the vibrational structure associated with the intermolecular stretching and bending motions. The reactive branching showed an anticorrelation with the bound-state resonances in the spectrum, suggesting a competition between the fast reaction and evaporation on the ground-state surface and a slower reaction on the excited-state surface.

Duncan and co-workers have studied the photodissociation of $Mg^+(CH_3OH)_n$, focusing on the spectroscopy of the monomer ($n = 1$), but they also examined the larger clusters at selected wavelengths.[2,3] For $Mg^+(CH_3OH)$, the dominant products are Mg^+ and $MgOH^+$, with a small branching to CH_3^+ and MgO^+. Broad vibronic structures were observed in the metal-based $3p\pi$-like excited states, and these were assigned to the Mg−O stretch motion. The spectroscopic evidence suggests that an intracluster solvation reaction to $MgOH^+$ or $MgOCH_3^+$ occurs in larger clusters near $n = 5$.

Farrar and co-workers also studied $Mg^+(CH_3OD)_n$ ($n = 1-5$) using photodissociation spectroscopy.[4] For the monomer $Mg^+(CH_3OD)$, the spectrum is broad and no vibrational structure was observed. The photodissociation-product branching ratios show strong selectivity as a function of cluster size that can be explained in terms of the initial photoexcited state, nonadiabatic couplings, and ground-state dissociation dynamics.

Very recently, Metz and co-workers examined the photodissociation spectroscopy of complexes formed when Fe^+ reacts with methanol.[5] Metz and co-workers found that a metal−hydroxo insertion complex $[HO-Fe-CH_3]^+$ can be formed in a laser vaporization source under certain experimental conditions. (This is in contrast with earlier reports by Schröder and co-workers, who found evidence only for the $Fe^+(CH_3OH)$ association complex in their experiments.)[6] Vibrational resonances were observed in the photodissociation action spectrum and assigned to the Fe−C and Fe−O stretch modes of the insertion complex in the excited state. The experimental results appear consistent with the theoretical calculations of the ground-state vibrational-mode frequencies. Together with earlier results on $Co(CH_3OH)^+$,[7] these observations suggest that there are notable differences in the chemistry of main-group-metal ions and that of transition-metal ions with methanol.

Here we report the photodissociation spectroscopy of Zn^+−methanol complexes. Zn^+ is a transition-metal ion with a closed $3d^{10}$ shell, making it spectroscopically similar to Mg^+. However, our results show a photodissociation action spectrum that is markedly different from that observed for $Mg^+(CH_3OH)$, exhibiting a sharp vibrational resonance structure with activity in both the inter- and intramolecular vibrational modes of the complex. Despite these differences, our experimental observations and theoretical calculations suggest that the complex is the simple association complex, $Zn^+(CH_3OH)$. The spectroscopic differences with other main-group-metal-ion−methanol complexes are a result of the relatively high first and second ionization energies of Zn, which lead to the opening of the low-energy charge-transfer reaction channels and a high activation barrier for the reaction to ZnOH products.

II. Experimental Arrangement

The experimental apparatus and the application to mass-selected cluster photodissociation spectroscopy measurements have been previously described.[8−10] $Zn^+(CH_3OH)$ complexes

* To whom correspondence should be addressed. E-mail: paul-kleiber@uiowa.edu.

10.1021/jp022028y CCC: $25.00 © 2003 American Chemical Society
Published on Web 01/23/2003

TABLE 1: Selected Structural Parameters for the $1^2A'$ and $2^2A'$ States of the Association Complex, $Zn^+(OHCH_3)$

	$1^2A'$			$2^2A'$
	UHF/ 6-311++g (2d,2p)	MP2/ 6-311++g (2d,2p)	B3LYP6/ 6-311++g (2d,2p)	UCIS/ 6-311++g (2d,2p)
D_e(Zn−O) (eV)	1.442	1.652	1.670	
R_e(Zn−O) (Å)	2.043	2.000	2.033	1.923
R_e(C−O) (Å)	1.453	1.476	1.478	1.465
θ(Zn−O−C) (deg)	129	129	129	131

were produced in the supersonic molecular beam expansion from a laser vaporization source. Methanol vapor was mixed at a level of about 2% in Ar. The seeded gas mix was then used in the pulsed gas valve at a backing pressure of 60 psi. The second harmonic of a pulsed Nd/yttrium aluminum garnet (YAG) laser was focused onto the metal rod surface and timed to overlap the seeded gas pulse.

Downstream from the source and molecular beam skimmer, ion clusters were pulse-extracted and accelerated into the flight tube of an angular reflectron time-of-flight mass spectrometer. A pulsed mass gate was used to select the $Zn^+(CH_3OH)$ parent cluster. The parent cluster was focused into the reflectron of the time-of-flight apparatus. The output from an injection-seeded Nd/YAG laser-pumped tunable optical parametric oscillator (OPO; Spectra-Physics/Quanta-Ray PRO-250/MOPL SL) coupled with a Quanta Ray WEX system for frequency doubling and mixing was time-delayed to excite the parent ion at the turning point inside the reflectron. The near-UV region from 212 to 345 nm was reached by frequency doubling the OPO output.

Parent and daughter fragment ions were then reaccelerated to an off-axis microchannel plate detector in a typical tandem time-of-flight arrangement. Two digital oscilloscopes, a multichannel scaler, and a set of gated integrators were used to monitor the mass spectrum and were interfaced to a laboratory personal computer to record the data for further analysis. The photodissociation action spectrum was determined by normalizing the daughter signal with respect to the parent-ion signal and laser power while scanning the laser wavelength. Results from a series of laser-power dependence tests were consistent with a one-photon excitation process. However, because of possible saturation effects for bound−bound transitions, we cannot entirely rule out multiphoton effects.

III. Theoretical Calculations

In view of the recent work of Metz and co-workers showing the formation of an insertion complex when Fe^+ reacts with methanol,[5] we have searched extensively for the possible isomers of $[Zn{-}CH_3OH]^+$. Calculations were performed using Gaussian 98.[11]

Ab initio calculations at the HF/6-311++g(2d,2p) level find two possible isomers.[12] The first is a direct association product of the form $Zn^+{-}OHCH_3$. This is a simple electrostatic complex with a nearly undistorted methanol ligand and a calculated Zn−O bond length R_e(Zn−O) = 2.04 Å and bond dissociation energy D_e''(Zn−O) = 1.442 eV at the HF level. The state is $1^2A'$ in C_s equilibrium geometry. Selected structural parameters are summarized in Table 1. Geometry optimization at the MP2/6-311++g(2d,2p) level gives a somewhat more strongly bound complex with an MP2 bond length R_e(Zn−O) = 2.00 Å and bond energy D_e''(Zn−O) = 1.652 eV.[13] Geometry optimization at the B3LYP/6-311++g(2d,2p) level[14] gives results very similar to the MP2 calculations. Again, the important structural parameters are summarized in Table 1.

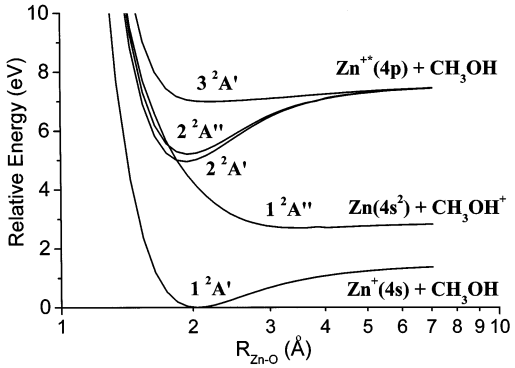

Figure 1. Calculated potential energy surfaces for several low-lying doublet states of $Zn^+(CH_3OH)$ at the HF/6-311++g(2d,2p) level. The excited states have been shifted to give the correct asymptotic energies.

The second "stable" structure we have identified is an insertion complex of the form $[HO{-}Zn{-}CH_3]^+$. This isomer is found at much higher energies, ∼1.81 eV above the energy of the association complex calculated at the same level of theory. Indeed, at the HF level the insertion complex lies ∼0.36 eV above the ground-state asymptote $Zn^+ + CH_3OH$. The results with density-functional theory show a slight improvement in stability. At the B3LYP/6-311++g(2d,2p) level we found a stable $[HO{-}Zn{-}CH_3]^+$ insertion isomer with a Zn−C bond length of 2.08 Å, a Zn−O bond length of 1.80 Å, and a C−Zn−O bond angle of 162°. At this level of theory, the insertion complex lies 1.44 eV above the energy of the association complex and is thus only weakly bound (by ∼0.23 eV) relative to the $Zn^+ + CH_3OH$ asymptote. We were not able to locate the corresponding transition state between the $[HO{-}Zn{-}CH_3]^+$ and $Zn^+ + CH_3OH$ isomers to determine the potential barrier to dissociation. However, given the obvious high energy of this isomer, we believe it is unlikely to be present in significant concentrations in our experiment. Coupled with the experimental observations (see below), we believe that the observed spectral features are most likely to result from the photodissociation of the simple association complex, $Zn^+(CH_3OH)$.

We have also used the single excitation configuration interaction method [CIS/6-311++g(2d,2p)] to study several low-lying excited states of $Zn^+(CH_3OH)$.[15] An ab initio calculation shows that the Zn^+-based 4p ← 4s transition will dominate the spectrum. In addition, because of the relatively high ionization energy of Zn (IE = 9.394 eV) and low IE of methanol (IE = 10.84 eV),[16] the charge-transfer state also lies at a low energy and is accessible in our experiment. Figure 1 shows the potential-energy surfaces for several low-lying excited states. This is a rigid-body scan obtained by varying only the Zn−O intermolecular bond length while keeping the other geometrical parameters fixed at their ground-state equilibrium values. We have found in previous work on several metal-ion−molecule complexes that the CIS method does a relatively good job of predicting the metal-ion-based excited states but a poor job of predicting the charge-transfer-based excited states.[8−10] Typically, metal-atom excited-state asymptotic energies are correct to within ∼0.5 eV, while the charge-transfer asymptotes are sometimes in error by several electronvolts.[10] For example, in $Zn^+(C_2H_4)$ we found that the experimental spectroscopic constants derived from an analysis of the Zn^+-based molecular band $1^2B_1(4p\pi) \leftarrow 1^2A_1(4s\sigma)$ are in excellent agreement with the CIS model predictions but that the CIS method predicts the charge-transfer band to lie at much higher energies than those experimentally observed. Nevertheless, our previous experience has shown that the CIS results can in some cases give valuable

TABLE 2: Experimental and Theoretical (in Parentheses) Vibrational Frequencies (cm^{-1}) for the $2^2A' \leftarrow 1^2A'$ Bands of $Zn^+(CH_3OH)$ and $Zn^+(CH_3OD)$

mode[a]	$Zn^+(CH_3OH)$	$Zn^+(CH_3OD)$	D/H ratio
υ_1: Zn−O−C out-of-plane bend	73 (64)	74 (64)	1.014 (0.998)
υ_2: Zn−O−C in-plane bend	243 (248)	243 (246)	1.000 (0.994)
υ_4: Zn−O stretch	511.7 (469)	495.7 (454)	0.969 (0.967)
υ_5: C−O stretch[b]	857 (874)	798 (818)	0.931 (0.936)
υ_6: CH_3 rock[b]	1094? (1086)	922 (943)	0.843 (0.868)

[a] The υ_3 CH_3-torsion mode with a predicted frequency of 400 cm^{-1} in $Zn^+(CH_3OH)$ was not observed. [b] The theoretical frequencies reported here for the intramolecular methanol vibrational modes have been scaled by 90% from the CIS-calculated results. See the text for an explanation.

qualitative (and even semiquantitative) insight into the excited-state structure and dynamics if the resulting potential curves are simply shifted in energy to agree with the known asymptotic energies.[10] This has been done in Figure 1 where the Zn^+-based excited states have been shifted up by 0.70 eV to give the correct Zn^+ 4p ← 4s atomic excitation of 6.08 eV[17] and the charge-transfer state has been shifted down in energy by 3.58 eV to give the correct asymptotic ionization-energy difference between Zn and CH_3OH of 1.45 eV. Obviously, the resulting potential-energy curves should be considered only as a qualitative guide to the discussion.

The ground state of $Zn^+(CH_3OH)$ is $1^2A'$ in C_s symmetry, correlating with the ground-state $Zn^+(4s\sigma) + CH_3OH$ asymptote. The lowest-energy excited state is expected to be the repulsive $1^2A''$ state that correlates asymptotically to the charge-transfer $Zn(4s^2) + CH_3OH^+$ products. The charge-transfer state is expected to cross the higher-lying $Zn^+(4p\pi)$-based excited states, and this interaction plays an important role in determining the excited-state chemistry.

There are three Zn^+*(4p)-based excited states at a higher energy resulting from the three different alignments of the Zn^+ 4p orbital with respect to the intermolecular axis. In the $2^2A'$-$(4p\pi)$ state, the Zn^+ p orbital lies in the symmetry plane but roughly perpendicular to the Zn−O bond. In the $2^2A''(4p\pi)$ state, the p orbital lies perpendicular to the symmetry plane. In the $3^2A'(4p\sigma)$ state, the p orbital lies in the symmetry plane and roughly along the Zn−O bond. Electrostatic arguments suggest that the $4p\pi$ states will be more strongly bound than the ground state because of the reduced electron density along the intermolecular axis. The corresponding absorption bands will be red-shifted from the bare Zn^+ 4p−4s atomic excitation at ∼204 nm. The calculated $2^2A'(4p\pi)$ and $2^2A''(4p\pi) \leftarrow 1^2A'$-$(4s\sigma)$ excitation energies are 5.02 (∼247.0 nm) and 5.25 eV (∼236.2 nm), respectively. (These are adjusted values to account for the asymptotic energy shift.) On the other hand, the $3^2A'$-$(4p\sigma)$ state should be less strongly bound than the ground state, owing to the increased electronic density along the intermolecular axis. The corresponding excitation band will be blue-shifted from the Zn^+ atomic excitation at 204 nm. The calculated (adjusted) $3^2A'(4p\sigma) \leftarrow 1^2A'(4s\sigma)$ excitation energy is 7.00 eV (∼177 nm) and is not readily accessible with our laser system.

Of particular interest here is the bound $2^2A'(4p\pi)$ state. We were able to optimize this excited-state geometry at the CIS/6-311++g(2d,2p) level. Optimization shows a more strongly bound excited-state complex with a shorter Zn−O bond length and a stretched C−O bond relative to the ground state. Structural parameters are summarized in Table 1. A frequency calculation gives results for several low-frequency vibrational modes of $2^2A'(4p\pi)$ (the intermolecular bending and stretching motions and the intramolecular C−O stretching and CH_3 rocking motions). The theoretical mode frequencies are given in Table 2 in parentheses. For comparison we also calculated the vibrational frequencies for isolated CH_3OH. For the corresponding intramolecular vibrational modes of methanol, the HF-level calculations overestimate the vibrational frequencies by ∼10% (ω_e = 1155 cm^{-1} calculated vs 1060 cm^{-1} experimental for the CH_3 rock and ω_e = 1164 cm^{-1} calculated vs 1033 cm^{-1} experimental for the C−O stretch).[18] This is consistent with the usual scaling of the HF vibrational frequencies by the "90% rule". In Table 2 we report the 90%-adjusted values for the CH_3 rock and C−O stretch frequencies. (Results from our previous work have shown that no such correction is usually necessary for the lower-energy intermolecular vibrational-mode frequencies, which are often well-predicted at the HF level.)[9,10] In Table 2 we also show analogous (adjusted) results for the deuterium-substituted isotope $^{64}Zn^+(CH_3OD)$.

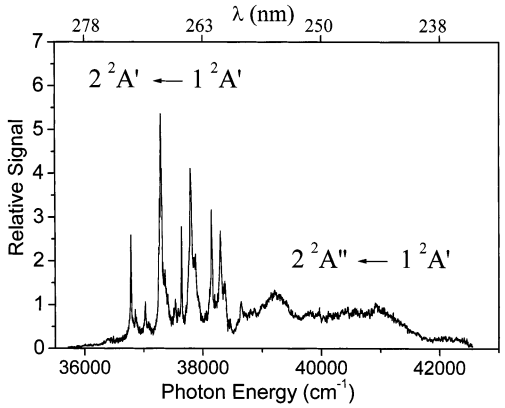

Figure 2. Photodissociation action spectrum for $Zn^+(CH_3OH)$ leading to CH_3OH^+. The spectra for CH_3^+ and Zn^+ are essentially the same.

IV. Results and Discussion

A. Band Assignment. The photodissociation action spectrum for Zn^+−methanol covers the near-UV region from ∼36 000 to ∼43 000 cm^{-1}. We observe three major products, including CH_3^+, CH_3OH^+, and Zn^+, with CH_3OH^+ being by far the most abundant (at >90% of the total yield). Figure 2 shows the action spectrum obtained by monitoring the major CH_3OH^+ product channel. The action spectra for CH_3^+ and Zn^+ are essentially the same. Figure 3 shows the photodissociation mass spectrum taken with the photolysis laser energy $h\nu$ = 36 782 cm^{-1}. The photodissociation of the deuterium-substituted complex $Zn^+(CH_3OD)$ gives CH_3^+, CH_3OD^+, and Zn^+ with a branching similar to the CH_3OH case.

The action spectrum shown in Figure 2 contains two overlapping bands. The lower-energy band, starting at 36 782 cm^{-1}, contains several sharp vibrational progressions and extends to around 39 000 cm^{-1}, while the higher-energy band appears as a nearly structureless continuum. An expanded view of the structured band is shown in Figure 4.

The low-energy band spectrum is very different from the spectra observed in the analogous Mg^+− or Sr^+−methanol complexes. Indeed, the spectral structure in this band bears a remarkable resemblance to the vibronic spectrum of $[HO-Fe-CH_3]^+$, studied by Metz and co-workers (see Figure 4 of ref 5).

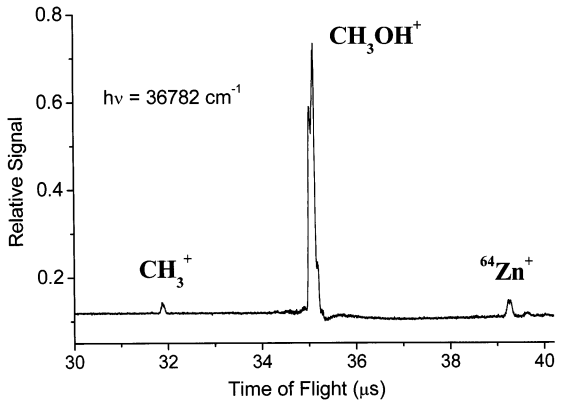

Figure 3. Photodissociation mass spectrum for $Zn^+(CH_3OH)$ taken with the photolysis laser tuned to the origin peak ($h\nu = 36\,782$ cm^{-1}).

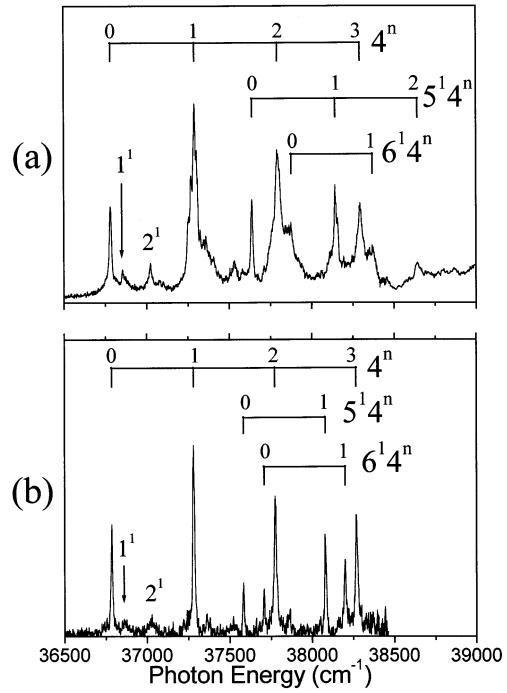

Figure 4. Expanded view of the $2^2A' \leftarrow 1^2A'$ band for (a) $Zn^+(CH_3OH)$ and (b) $Zn^+(CH_3OD)$.

On the basis of this similarity, we originally thought our structured band could be assigned to a transition in the corresponding Zn insertion complex, $[HO-Zn-CH_3]^+$. However, on the basis of the theoretical ab initio results described above and a detailed analysis of the experimental results, we now believe that the spectral similarity to the Fe metal−hydroxo insertion complex is simply a curious coincidence. We instead assign the lower-energy structured band to the Zn^+-based $2^2A'(4p\pi) \leftarrow 1^2A'(4s\sigma)$ transition.

This band assignment is based on several factors. First, the ab initio calculations find that the insertion isomer is much higher in energy and only very weakly bound in comparison to the association complex. It is difficult to understand how we could find such a strong absorption signal from the insertion isomer. Second, the CIS-level calculations predict only very weak transitions ($f \leq 10^{-3}$) from the insertion complex in the near UV, whereas we see quite strong absorption bands consistent with a strong Zn^+-based radiative transition. Third, the observed vibrational resonance structure and isotope shifts are in quite good agreement with the CIS predictions for the association complex (vide infra) but not with predictions for the insertion complex. Finally, we observe CH_3OH^+ as the dominant dissociation product with a yield > 90%. This observation is easy to explain for the photodissociation of the association complex but much harder to explain for the photodissociation of a $[HO-Zn-CH_3]^+$ insertion isomer because it would require significant rearrangement of the complex before dissociation.

TABLE 3: Observed Vibrational Resonances for the $2^2A' \leftarrow 1^2A'$ Band of $Zn^+(CH_3OH)$

peak position (cm^{-1})[a]	assignment[b]	peak position (cm^{-1})[a]	assignment[b]
36 782 (36 786)	0^0	37 793 (37 774)	4^2
36 855 (36 860)	1^1	37 876? (37 708)	6^1
37 025 (37 029)	2^1	38 143 (38 078)	$5^1 4^1$
37 290 (37 281)	4^1	38 293 (38 267)	4^3
37 359 (37 358)	$4^1 1^1$	38 369 (38 200)	$6^1 4^1$
37 532 (37 521)	$4^1 2^1$	38 643	$5^1 4^2$
37 639 (37 584)	5^1		

[a] Results for $Zn^+(CH_3OD)$ are given in parentheses. [b] υ_1: Zn−O−C out-of-plane bend. υ_2: Zn−O−C in-plane bend. υ_4: Zn−O stretch. υ_5: C−O stretch. υ_6: CH_3 rock.

The higher-energy band starts at around 38 500 cm^{-1} and extends up to ~43 000 cm^{-1}. The origin of this band is not obvious because of overlap with the lower-energy band. This band is assigned to the Zn^+-based $2^2A''(4p\pi) \leftarrow 1^2A'(4s\sigma)$ transition. This band does not show obvious vibrational structure, although several broad humps are apparent. We suspect that the structureless nature of this band is due to a strong coupling between the metal-based $2^2A''(4p\pi)$ state and the lower-lying repulsive $1^2A''$ charge-transfer state of the same symmetry resulting in a fast predissociation.

B. Vibrational Analysis of the $2^2A'(4p\pi) \leftarrow 1^2A'(4s\sigma)$ Band. The metal-based $2^2A'(4p\pi) \leftarrow 1^2A'(4s\sigma)$ band exhibits several sharp vibrational progressions (Figure 4) with the resonance peaks shown in Table 3. To help clarify the vibrational assignment, we have also studied the deuterium-substituted complex, $Zn^+(CH_3OD)$, and the results are also shown in Figure 4 and summarized in Table 3. We note that the vibrational features in the spectrum of $Zn^+(CH_3OD)$ are substantially sharper than those of $Zn^+(CH_3OH)$, although the reason for this is not entirely clear. The experimental conditions for these two systems are essentially the same, and the parent cluster ions are likely to be at a similar temperature. The difference may be related to the different rotational contours for $Zn^+(CH_3OH)$ and $Zn^+(CH_3OD)$, although we do not resolve any rotational structure.

The first observed resonance for $Zn^+(CH_3OH)$ at 36 782 cm^{-1} is assigned to the 0_0^0 origin peak. The origin shows only a small isotope shift to 36 786 cm^{-1} for $Zn^+(CH_3OD)$. To the red of the first strong peak we find no identifiable resonance features, suggesting that this is the true origin. There is, however, a weak bump near 36 400 cm^{-1} that can be assigned to a hot band. The vibrational spacing for the hot band is 382 cm^{-1}, and it is assigned to a single quantum of the Zn−O stretch in the ground state of $Zn^+(CH_3OH)$. The calculated frequency for the ground-state intermolecular stretch is 337 cm^{-1}.

The spectrum of $Zn^+(CH_3OH)$ shown in Figure 4a shows an obvious progression built on the origin with a spacing of ~500 cm^{-1}. This progression is assigned to the a' Zn−O stretch mode (υ_4) with a CIS-calculated frequency of 469 cm^{-1}. Birge−Sponer analysis gives the fundamental frequency for this mode as $\omega_4' = 511.7 \pm 1.2$ cm^{-1} with an anharmonicity parameter $\omega_e x_e' = 2.0 \pm 0.3$ cm^{-1}.

There is another short but obvious progression in the υ_4 mode built on an origin at 37 639 cm^{-1} = 0_0^0 + 857 cm^{-1}. The

progression is assigned to a combination band with one quantum of the a' C−O stretch (υ_5). The C−O stretch frequency of $\omega'_5 = 857$ cm^{-1} is in very good agreement with the calculated frequency of 971 cm^{-1} if the theoretical result is scaled by the 90% rule. This frequency is decreased from that of the free CH_3OH molecule (1033 cm^{-1}), and this is consistent with the ab initio predictions that suggest a stronger and shorter Zn−O bond and weaker and longer C−O bond in this excited state of the complex.

There are other weak features in the spectrum as well. Two small peaks to the high-energy side of the band origin at $0_0^0 +$ 73 cm^{-1} and $0_0^0 +$ 243 cm^{-1} can be assigned to the a'' Zn−O−C out-of-plane bend (υ_1) with a calculated frequency of 64 cm^{-1} and the a' Zn−O−C in-plane bend (υ_2) with a calculated frequency of 248 cm^{-1}, respectively. These two modes also appear on the high-energy side of the 4_0^1 peak. There is probably one additional weak, short progression in the υ_4 mode built on an origin at roughly $0_0^0 +$ 1094 cm^{-1}. This origin is tentatively assigned to one quantum of the a' CH_3 rocking mode (υ_6) with a calculated frequency of 1207 cm^{-1}. The peak position is not very accurate because of the overlap with the nearby strong υ_4 progression, but it is more well-resolved in the case of $Zn^+(CH_3OD)$. Again, the agreement with the CIS prediction is very good if we scale the theoretical results by 90%. The experimental mode frequencies are listed in Table 1 and compared with the CIS-model predictions for the $2\ ^2A'$ state of $Zn^+(CH_3OH)$.

The vibrational structure in $Zn^+(CH_3OD)$ shown in Figure 4b can be assigned in a similar way. Birge−Sponer analysis gives the fundamental Zn−O intermolecular stretch frequency as $\omega_4' = 495.7 \pm 1.2$ cm^{-1}, with an anharmonicity parameter $\omega_e x_e' = 0.50 \pm 0.29$ cm^{-1}. This mode shows an isotopic ratio of $\omega_4(D)/\omega_4(H) = 0.969$, and this is in excellent agreement with the calculated ratio of 0.967 (Table 1). The C−O stretch-mode frequency for $Zn^+(CH_3OD)$ is found to be $\omega_5' = 798$ cm^{-1}, which can be compared with the calculated value of 909 cm^{-1}. The corresponding isotopic ratio of 0.931 is also in excellent agreement with the calculated value of 0.936. The υ_6−CH_3 rocking mode, with an experimental frequency of $\omega_6' = 922$ cm^{-1}, shows a large isotopic effect with a D/H ratio of 0.843 that is also in good agreement with the CIS-model predictions for this mode. Similarly, the experimental results for the bending modes of $Zn^+(CH_3OD)$ are found to be $\omega_1' = 74$ cm^{-1} and $\omega_2' = 243$ cm^{-1} for the out-of-plane and in-plane modes, respectively. Again, these results are summarized in Table 1.

The experimental vibrational frequencies are in good agreement with the calculated ones, and the agreement for the isotope shifts is excellent. These results are consistent with our assignment of the observed spectrum for the $Zn^+(CH_3OH)$ association complex. (For the possible insertion complex $[OH-Zn-CH_3]^+$, we were not able to find a bound excited state. The corresponding ground-state complex shows a large number of low-frequency vibrations, but the match with the experimental results is not good.)

C. Discussion. The photodissociation action spectrum for $Zn^+(CH_3OH)$ is quite different from that observed previously for $Mg^+(CH_3OH)$. In particular, the $2^2A'(4p\pi) \leftarrow 1^2A'(4s\sigma)$ band in Figure 4 shows a much more clearly resolved vibronic structure, suggesting that the $2^2A'$ state is longer-lived and less distorted in the Zn^+ case. In contrast, the higher-energy $2^2A''$ $(4p\pi) \leftarrow 1^2A'(4s\sigma)$ band appears to show a less detailed structure than the corresponding band in $Mg^+(CH_3OH)$ (compare with Figure 3 of ref 3). Additionally, for $Zn^+(CH_3OH)$ the dominant dissociation product is the charge-transfer product, CH_3OH^+. We observe very little dissociation to reactive product channels. For $Mg^+(CH_3OH)$, on the other hand, the reactive dissociation to $MgOH^+ + CH_3$ was a major decay channel.

These differences in the Zn case are probably due to its relatively high first and second ionization energies. Because of the high first ionization energy, the $1^2A''$ charge-transfer state lies at a low energy and is expected to cross the Zn^+*$(4p\pi)$-based excited states at short internuclear distances (Figure 1). The $1^2A''-2^2A'$ crossing may occur at an energy somewhat above the $2^2A'$-state minimum. In C_s geometry, these states do not couple because they have different symmetries. Thus, $2^2A'$ is expected to be long-lived (with respect to the charge-transfer dissociation) and can show a sharp resonance structure. This assumes that the complex retains C_s symmetry with one of the methyl H atoms lying in the plane of the heavy atoms. Because this only involves a hindered rotation of the methyl group, the symmetry restriction may be relaxed and some $1^2A''-2^2A'$ coupling might be possible. However, on the basis of the spectroscopy, this coupling appears to be weak for the low vibrational levels in $2^2A'$. The nonadiabatic coupling rate may become larger at higher vibrational energies, above the curve crossing and where the distortion away from C_s symmetry may be more pronounced, leading to a relatively short vibrational progression as observed. On the other hand, we expect strong coupling between the $1^2A''$ and $2^2A''$ states, leading to an avoided surface crossing. In this spectral region, the states are probably of strongly mixed metal excited and charge-transfer character, leading to a fast charge-transfer dissociation. In $Mg^+(CH_3OH)$, the charge-transfer state lies at a much higher energy, and the corresponding charge-transfer dissociation channel is not energetically accessible.

In previous studies of the photodissociation of metal-ion−methanol complexes, the reactive dissociation to $MeOH^+$ products was a major decay channel.[1−5] In contrast, here we see very low branching to the reactive product channels, $ZnOH^+ + CH_3$ or $CH_3^+ + ZnOH$, despite the fact that these channels are certainly energetically open. (After all, we do see some CH_3^+ as a reactive product.) To the best of our knowledge, the bond energies for ZnOH and $ZnOH^+$ are not known. However, if we assume that these bond energies are comparable to those for MgOH and $MgOH^+$, respectively, we estimate the energetic (spectroscopic) thresholds for these channels to be

$$Zn^+(CH_3OH) + h\nu \rightarrow ZnOH + CH_3^+ \qquad \Delta E \sim 1.86 \text{ eV } (\lambda = 666 \text{ nm})$$

$$\rightarrow ZnOH^+ + CH_3 \qquad \Delta E \sim 2.45 \text{ eV } (\lambda = 505 \text{ nm})$$

While these assumptions may be somewhat in error, it seems unlikely that the estimated thresholds are in error by enough to explain the very weak observed reactive branching in $Zn^+(CH_3OH)$ on the basis of the energetics alone.

The weak reactive branching might be due in part to competition with the fast nonreactive charge-transfer dissociation process. However, even in the relatively long-lived $2^2A'$ state, we see a very small reactive branching in comparison to that of the $Mg^+(CH_3OH)$ case.[3] Our results suggest that there may be a larger activation barrier to the reaction in $Zn^+(CH_3OH)$ than to that in $Mg^+(CH_3OH)$. The origin of this difference is not obvious given the similar electronic valence character and excited structure and energetics of Mg^+ and Zn^+. A larger activation barrier might be expected for $Zn^+ + CH_3OH$ reactions because of the relatively higher second ionization energy of Zn [IE(Zn^+) = 18.0 eV compared to IE(Mg^+) = 15.0 eV]. If the

reaction proceeds through a transition state that has some formal charge-transfer character, the energy to access this transition state may be higher in the Zn case, resulting in a larger activation barrier to the reaction.

The photodissociation of a weakly bound bimolecular complex can serve to mimic a bimolecular "half-collision" and give insight into the collision dynamics. In this "half-collision" model, our results suggest that the collisional quenching of Zn^+*(4p) by methanol will occur primarily through charge transfer rather than by a reaction to metal hydroxide products.

Acknowledgment. We gratefully acknowledge the National Science Foundation for support of this research through Grant CHE-9982119.

References and Notes

(1) Qian, J.; Midey, A. J.; Donnelly, S. G.; Lee, J. I.; Farrar, J. M. *Chem. Phys. Lett*. **1995**, *244*, 414.

(2) Yeh, C. S.; Willey, K. F.; Robbins, D. L.; Duncan, M. A. *Int. J. Mass Spectrom. Ion Processes* **1994**, *131*, 307.

(3) France, M. R.; Pullins, S. H.; Duncan, M. A. *Chem. Phys*. **1998**, *239*, 447.

(4) Lee, J. I.; Sperry, D. C.; Farrar, J. M. *J. Chem. Phys*. **2001**, *114*, 6180.

(5) Aguirre, F.; Husband, J.; Thompson, C. J.; Stringer, K. L.; Metz, R. B. *J. Chem. Phys*. **2002**, *116*, 4071.

(6) Schröder, D.; Fiedler, A.; Hrušák, J.; Schwarz, H. *J. Am. Chem. Soc*. **1992**, *114*, 1215.

(7) Chen, Y. M.; Clemmer, D. E.; Armentrout, P. B. *J. Am. Chem. Soc*. **1994**, *116*, 7815.

(8) Kleiber, P. D.; Chen, J. *Int. Rev. Phys. Chem*. **1998**, *17*, 1.

(9) Kleiber, P. D. In *Advances in Metal and Semiconductor Clusters*; Duncan, M. A., Ed.; JAI Press: New York, 2001; Vol. 5, p 267.

(10) Lu, W.-Y.; Kleiber, P. D.; Young, M. A.; Yang, K.-H. *J. Chem. Phys.* **2001**, *115*, 5823.

(11) Frisch, M. J.; Trucks, G. W.; Schlegel, H. B.; et al. *Gaussian 98*, Revision A.6; Gaussian, Inc.: Pittsburgh, PA, 1998.

(12) Pople, J. A.; Nesbet, R. K. *J. Chem. Phys*. **1959**, *22*, 571.

(13) Moller, C.; Plesset, M. S. *Phys. Rev*. **1934**, *46*, 618.

(14) Becke, A. D. *J. Chem. Phys*. **1993**, *98*, 5648.

(15) Foresman, J. B.; Head-Gordon, M.; Pople, J. A.; Frisch, M. J. *J. Phys. Chem*. **1992**, *96*, 135.

(16) Lias, S. G. Ionization Energy Evaluation. In *NIST Chemistry WebBook*; Linstrom, P. J., Mallard, W. G., Eds.; NIST Standard Reference Database Number 69; National Institute of Standards and Technology: Gaithersburg, MD, July 2001 (http://webbook.nist.gov).

(17) Moore, C. E. *Atomic Energy Levels*; NSRDS-NBS 35; U.S. Department of Commerce: Washington, DC, 1971; Vol. I.

(18) Shimanouchi, T. Molecular Vibrational Frequencies. In *NIST Chemistry WebBook*; Linstrom, P. J., Mallard, W. G., Eds.; NIST Standard Reference Database Number 69; National Institute of Standards and Technology: Gaithersburg, MD, July 2001 (http://webbook.nist.gov).